SUPPLEMENTAL MATERIAL

von Willebrand Factor unfolding and elongation on collagen during acute whole blood exposure to pathological flow

T. V. Colace and S. L. Diamond

Institute for Medicine and Engineering

1024 Vagelos Research Laboratory

University of Pennsylvania

Philadelphia, PA 19104

215-573-5702

sld@seas.upenn.edu

Supplemental Discussion

A velocity field **v**(*x,y,z*) can be represented as the superposition of two components: its vorticity $\boldsymbol{\omega}$ (which only rotates a collapsed polymer) and deformation **D** (which extends and compresses a collapsed polymer) where the elongation rate $\dot{\mathbf{e}}$ = *grad* **v** = $\boldsymbol{\omega}$ + **D**.1 In theory, a cone-and-plate viscometer creates an ideal linear shear field that is both rotational and deformational. In cone-and-plate viscometers, we note that the collision rate between vWF molecules and the unavoidable generation of secondary flows due to fluid inertia are both greatly enhanced when pathological shear rates are obtained.2 In contrast to a linear shear field, flow acceleration into and deceleration out of a stenosis creates an elongational flow with significant hydrodynamic forces that are expected to cause coil-stretch transitions in polymers in the bulk flow.3′4 Impinging and contracting flows, boundary layer separation, and vortexing secondary flows may also generate significant elongational forces to alter vWF conformation in a flow field. Distinct from these situations is unidirectional and parabolic viscous flow over a surface as encountered in pipe flow or flow between parallel-plates. Very near the surface (eg. < 400 nm for globular vWF with a prolate ellipsoid shape of 175 x 28 nm for multimeric vWF),5 the boundary layer flow approximates a linear shear field. In this region very near the wall, a strong linear shear field can cause vWF to rotate and experience oscillatory compression and extension as it rotates. However, a linear shear field of sufficient strength is likely to only cause flow-alignment, but is unlikely to generate significant stretching of polymer molecules.1 In contrast, an accelerating flow that is highly elongational is best suited to cause an extended and stretched vWF conformation in the bulk flow away from the wall.6

At sufficiently high γ_w the process of vWF unfolding *on the wall* occurs for plasma or whole blood flow where the wall shear rate is not changing in the direction of flow ($grad_x\ \gamma_w = 0$) for a constant-width microfluidic device completely lacking a stenotic inlet (**Fig. S4-5**). Theoretical treatments of adsorbed polymer extension on a wall are just emerging7′8 and indicate fundamental differences from processes in bulk flow. The vWF adsorption problem include difficult aspects of: (1) adsorption-driven annealing of vWF to multimeric collagen; (2) sub-micron geometries and flow fields (with non-zero $\boldsymbol{\omega}$ and **D**) around molecules of finite submicron size such as globular vWF and fibrillar collagen; (4) hydrodynamic interactions of the partially adsorbed molecule with the wall, and (4) quantifying sub-nanometer water movement around and through a porous and extending vWF protein. Such theories also require an estimate of the vWF relaxation time λ, however, it is unclear if relaxation rates measured for vWF bundles apply to single vWF multimers.9 While micron-scale gradients in a microfluidic flow field are not required for elongated vWF fiber formation on collagen, we show that pathological wall shear rates are highly predictive of their formation. The role of sub-micron flow fields that change on the length scale of a single protein or collagen fiber (or individual platelet) and may create elongational forces remains an area of investigation.

Supplemental References

1. Smith DE, Babcock HP, Chu S. Single-polymer dynamics in steady shear flow. *Science*. 1999;283:1724-1727.
2. Shankaran H, Neelamegham S. Effect of secondary flow on biological experiments in the cone-plate viscometer: Methods for estimating collision frequency, wall shear stress and inter-particle interactions in non-linear flow. *Biorheology*. 2001;38:275-304.
3. De Gennes PG. Coil-stretch transition of dilute flexible polymers under ultrahigh velocity gradients. *J Chem Phys.* 1974;60:5030-5042.
4. Sing CE, Alexander-Katz A. Elongational flow induces the unfolding of von Willebrand factor at physiological flow rates. *Biophys J*. 2010;98:L35-L37.
5. Singh I, Shankaran H, Beauharnois ME, Xiao Z, Alexandridis P, Neelamegam S. Solution structure of human von Willebrand factor studied using small angle neutron scattering. *J Biol Chem*. 2006;281:38266-38275.
6. Sing CE, Alexander-Katz A. Dynamics of collapsed polymers under the simultaneous influence of elongational and shear flows. *J Chem Phys*. 2011;135:014902-1-14.
7. He GL, Messina R, Lowen H. Statistics of polymer adsorption under shear flow. *J Chem Phys*. 2010;132:124903-1-10.
8. Sing CE, Alexander-Katz A. Theory of tethered polymers in shear flow: The strong stretching limit. *Macromolecules.* 2011;44:9020-9028.
9. Steppich DM, Angerer JI, Sritharan K, Schnieder SW, Thalhammer S, Wixforth A, Alexander-Katz A, Schneider MF. Relaxation of ultralarge VWF bundles in a microfluidic-AFM hybrid reactor. *Biochem Biophys Res Commun.*2008;369:507-512.

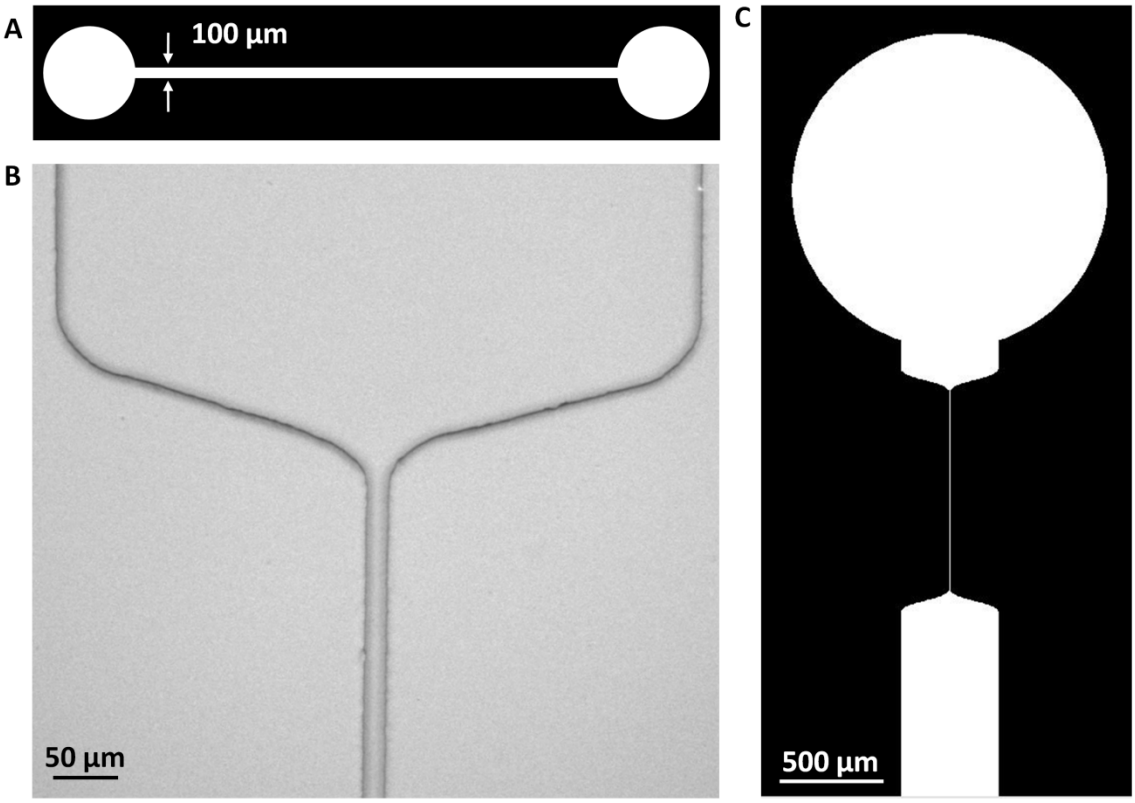

Supplemental Figure I, The straight channel microfluidic device used in this study had a constant cross section of 100 µm wide by 60 µm tall. The large circles at the ends of the channel are the inlet/outlet ports. **B,** A bright field micrograph of the inlet to the stenosis in the stenosis channel. At the top of the image the channel cross section is 500 µm wide by 60 µm high. The channel rapidly tapers over a 100 µm length to a 15 µm wide by 60 µm high region. **C,** This representation of the stenosis channel illustrates that the 15 µm wide stenosis region was 1 mm in length.

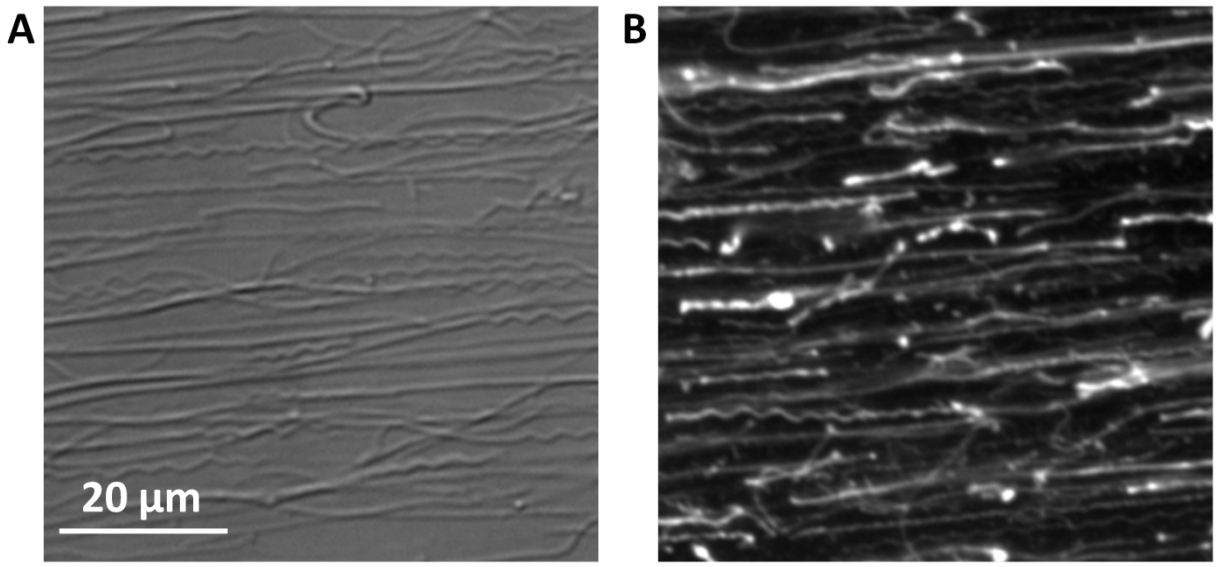

Supplemental Figure II A, A representative bright field image of the collagen type 1 coated surface used in this study. **B,** A representative fluorescence microscopy image of a collagen type 1 surface treated with a biotinylated polyclonal anti-collagen antibody and fluorescently labeled streptavidin.

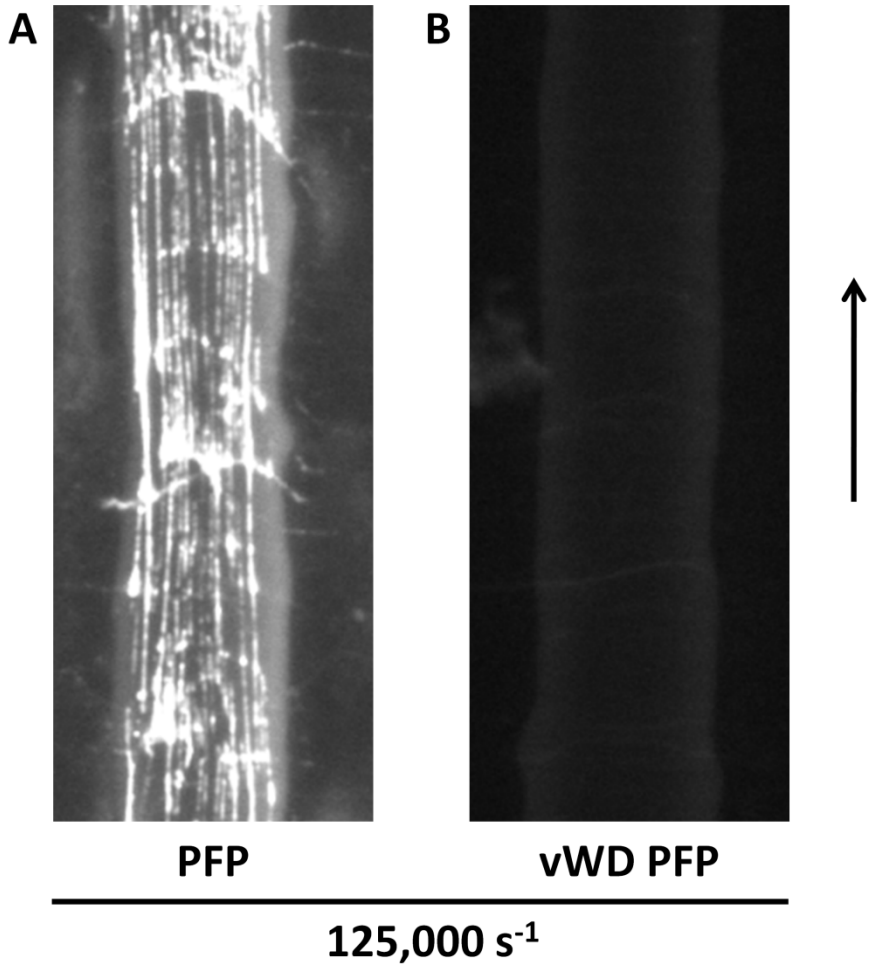

Supplemental Figure III, Plasma from a patient with severe von Willebrand disease does not deposit vWF fibers. **A,** PFP (EDTA) was perfused over a collagen type 1 surface in the stenosis chamber at the indicated wall shear rate. vWF fibers are detected using a fluorescently labeled polyclonal antibody. **B,** Plasma from a patient with severe vWD was also treated with EDTA and perfused in a similar manner as **A**. No vWF fibers are detected.

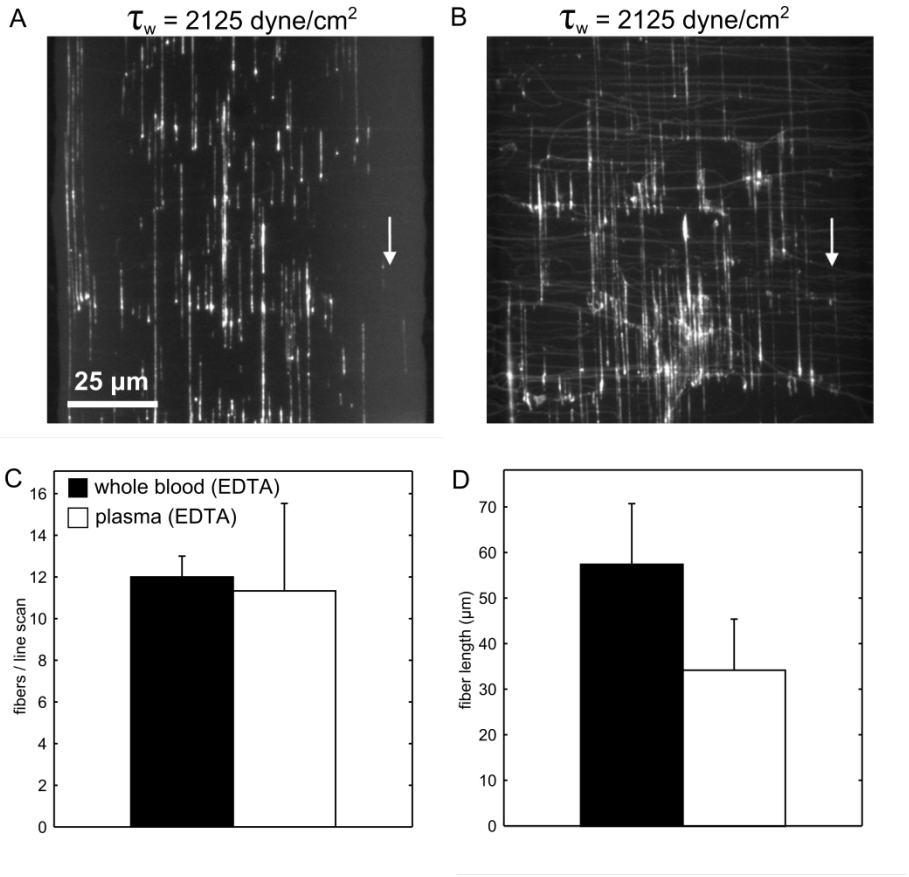

Supplemental Figure IV, Whole blood (EDTA) treated with a function blocking antibody against GPIb (A) or plasma (EDTA) was perfused over a collagen type 1 surface in a microfluidic channel of constant cross section (100 µm by 60 µm). Given the width of the channel, collagen was briefly fixed for 30 s with 2 % glutaraldehyde to help attach it to the surface. The centerline wall shear rate was 48,000 s^{-1} for the whole blood sample and 125,000 s^{-1} for the plasma sample to maintain constant wall shear stress (τ_w = 2125 dyne/cm^2). The surfaces were washed after sample perfusion and stained for vWF, images are representative of at least 3 experiments per condition. **A,B** Fibers of vWF are observed in both conditions in these representative images. **C,** The mean number of fibers (n=3) intersecting a line scan drawn horizontally through the center of the image was counted for each condition. **D,** The length of each of the fibers intersecting the line scan from **C** was averaged for each condition.

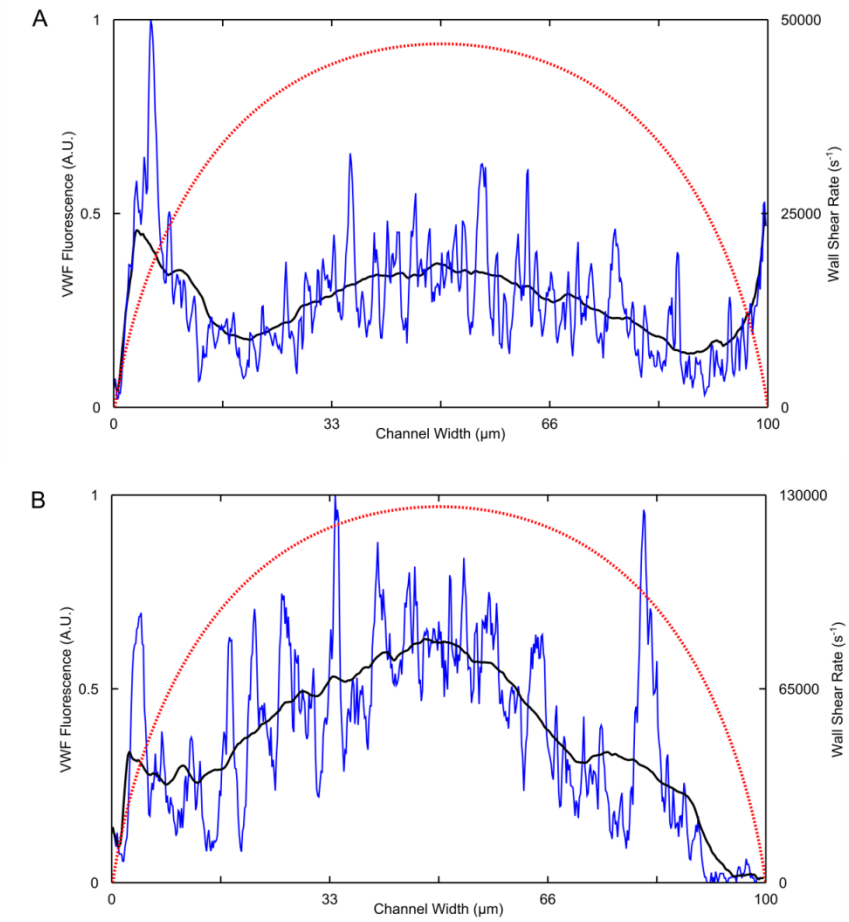

Supplemental Figure V, vWF fluorescence for whole blood (EDTA) treated with a function blocking antibody against GPIb (**A**) or plasma (EDTA) (**B**) perfused over a collagen type 1 surface in a channel of constant cross section (100 μm by 60 μm). The centerline wall shear rate was 48,000 s^{-1} for the whole blood sample and 125,000 s^{-1} for the plasma sample to maintain constant wall shear stress (τ_w = 2125 dyne/cm^2). The vWF fluorescence over the channel width was averaged over the length of the viewing window for 3 replicates (blue line) and was mathematically smoothed (black line). The dashed red lines indicate the local wall shear rate along the 100 μm width as calculated from the analytical solution for the velocity profile in a rectangular duct. **A,** vWF fluorescence is elevated in the middle of the channel where the wall shear rate is at a maximum. In the corners, high signal was also observed (especially in the case of whole blood flow), which may be due to the non-physiologic corner-flow geometry of the device. **B,** In plasma samples, the highest signal was observed along the center of the channel.

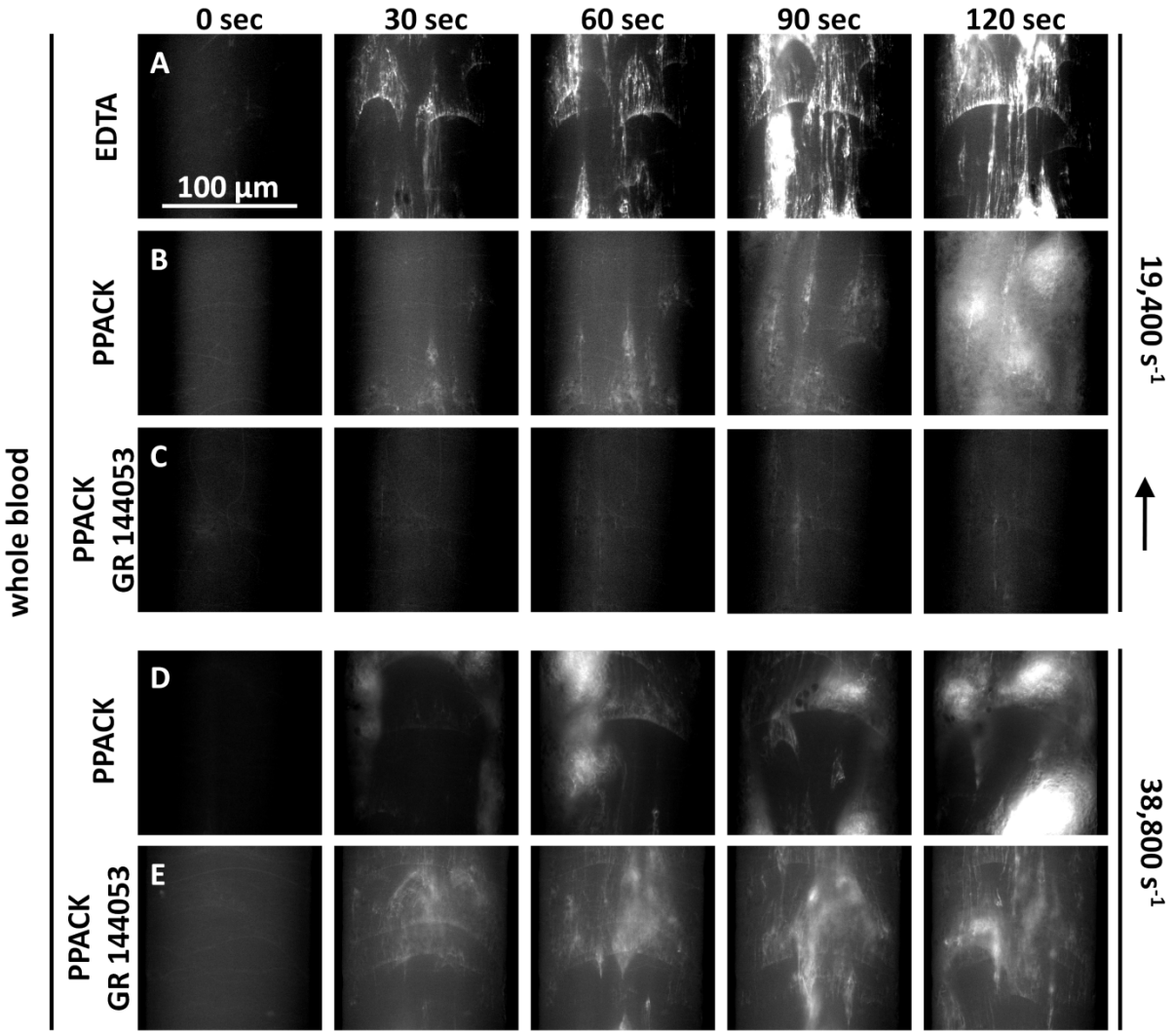

Supplemental Figure VI A, EDTA-treated whole blood was perfused over a collagen type 1 surface in a microfluidic channel with a 100 µm x 60 µm cross section at the indicated wall shear rate. Within 30 sec, long fibers of vWF were seen on the surface. Shortly after, rolling aggregates of platelets and vWF were observed. **B,** PPACK-treated whole blood was perfused in an identical manner as **A**. vWF fibers were detected after 30 sec, although there was less deposition. By two minutes massive platelet aggregation had occurred. **C,** The $\alpha_{IIb}\beta_3$ inhibitor, GR 144053, was used to prevent massive platelet aggregation in an identical perfusion experiment to **A**. Reduced vWF deposition was observed under these conditions, suggesting a role for $\alpha_{IIb}\beta_3$-mediated platelet adhesion in supporting vWF fiber elongation and aggregation. **D,E,** Identical experiments to **B and C** were performed at 2-fold increased wall shear rate. The deposition of vWF was markedly increased. The time to platelet aggregation was also reduced.

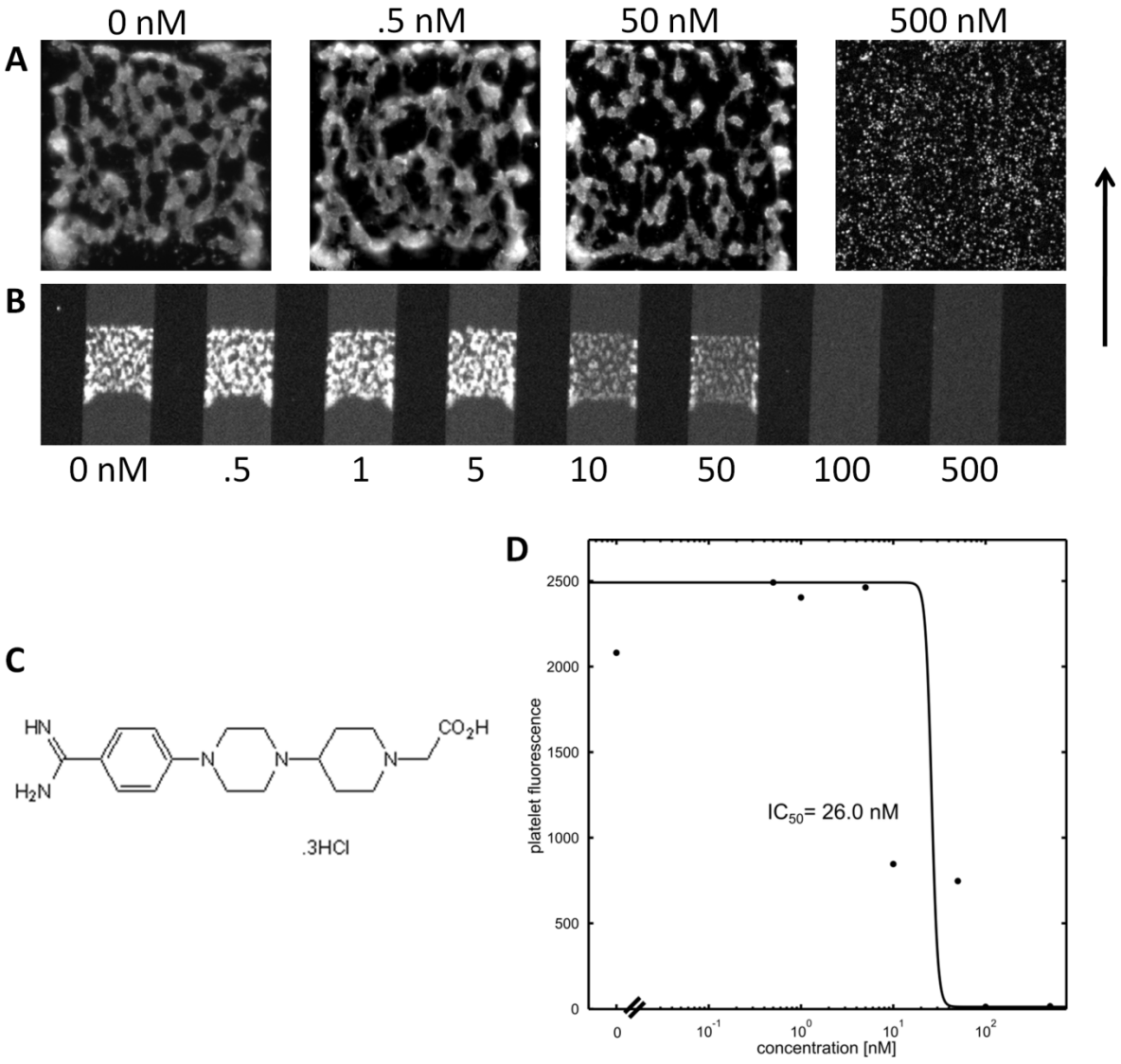

Supplemental Figure VII, Compound GR 144053 inhibits secondary platelet aggregation on collagen type 1 surfaces. **A,** Fluorescently labeled platelets in WB (PPACK) were perfused over a collagen type 1 surface at 200 s^{-1} in the presence of the indicated amount of GR 144053. **B,** The perfusion experiment was performed in an 8-channel microfluidic device that allowed for 8 different inlet concentrations of the inhibitory compound. **C,** A representation of the chemical structure of GR 144053 (provided by Tocris Bioscience). **D,** The platelet fluorescence after 5 minutes of perfusion over a collagen type-1 surface in the 8 channel microfluidic device was used to obtain an IC_{50} value for GR 144053, 26.0 nM.

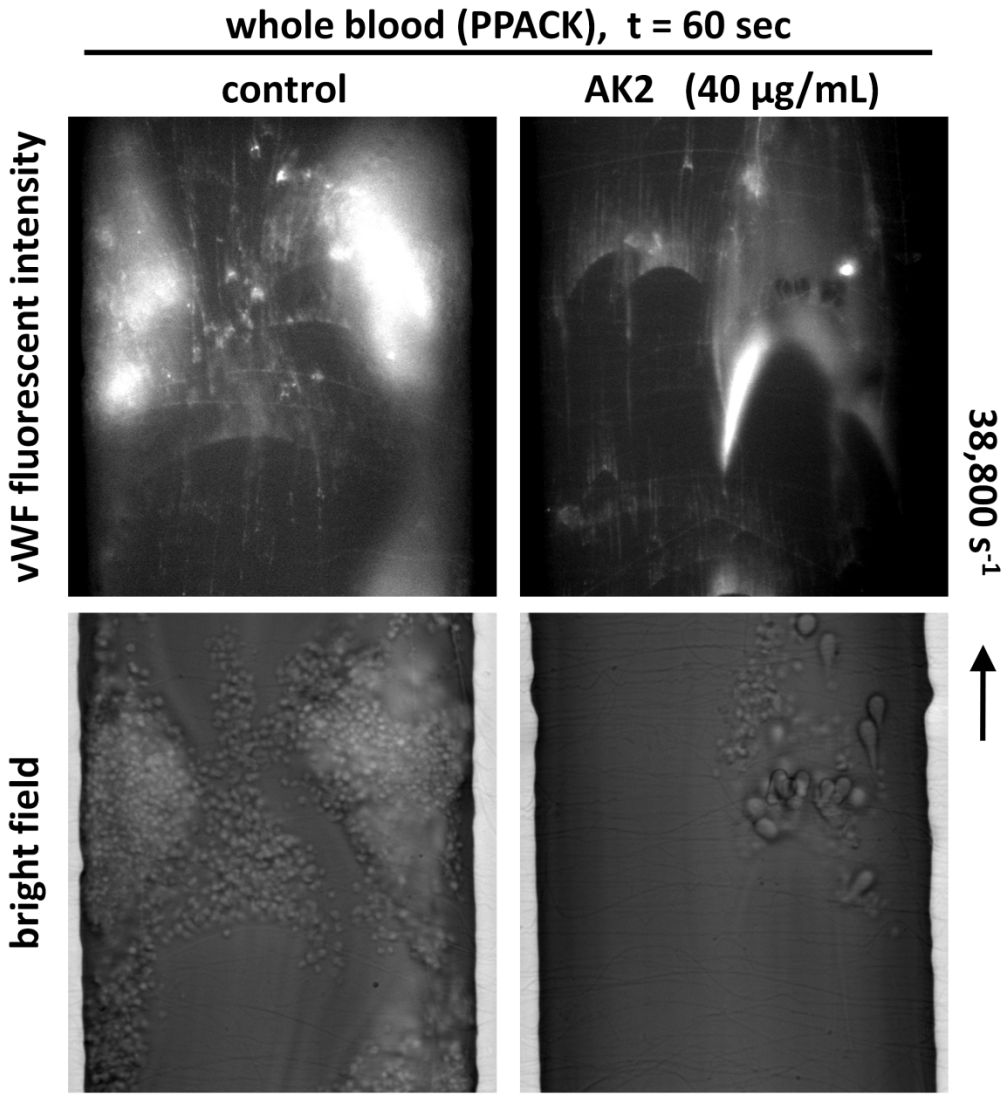

Supplmental Figure VIII, The formation of stable platelet adhesion and platelet aggregates required GPIb/vWF interaction**.** Whole blood in the presence or absence of 40 µg/mL of function blocking anti-GPIb antibody, AK2, was perfused at the indicated wall shear rate over a collagen type 1 surface. Under both conditions vWF deposition was observed. In the presence of the neutralizing antibody, few platelets firmly adhered to the surface while many were seen in its absence. Furthermore, large platelet aggregates were present in the absence of AK2. The images are representative of multiple experiments.

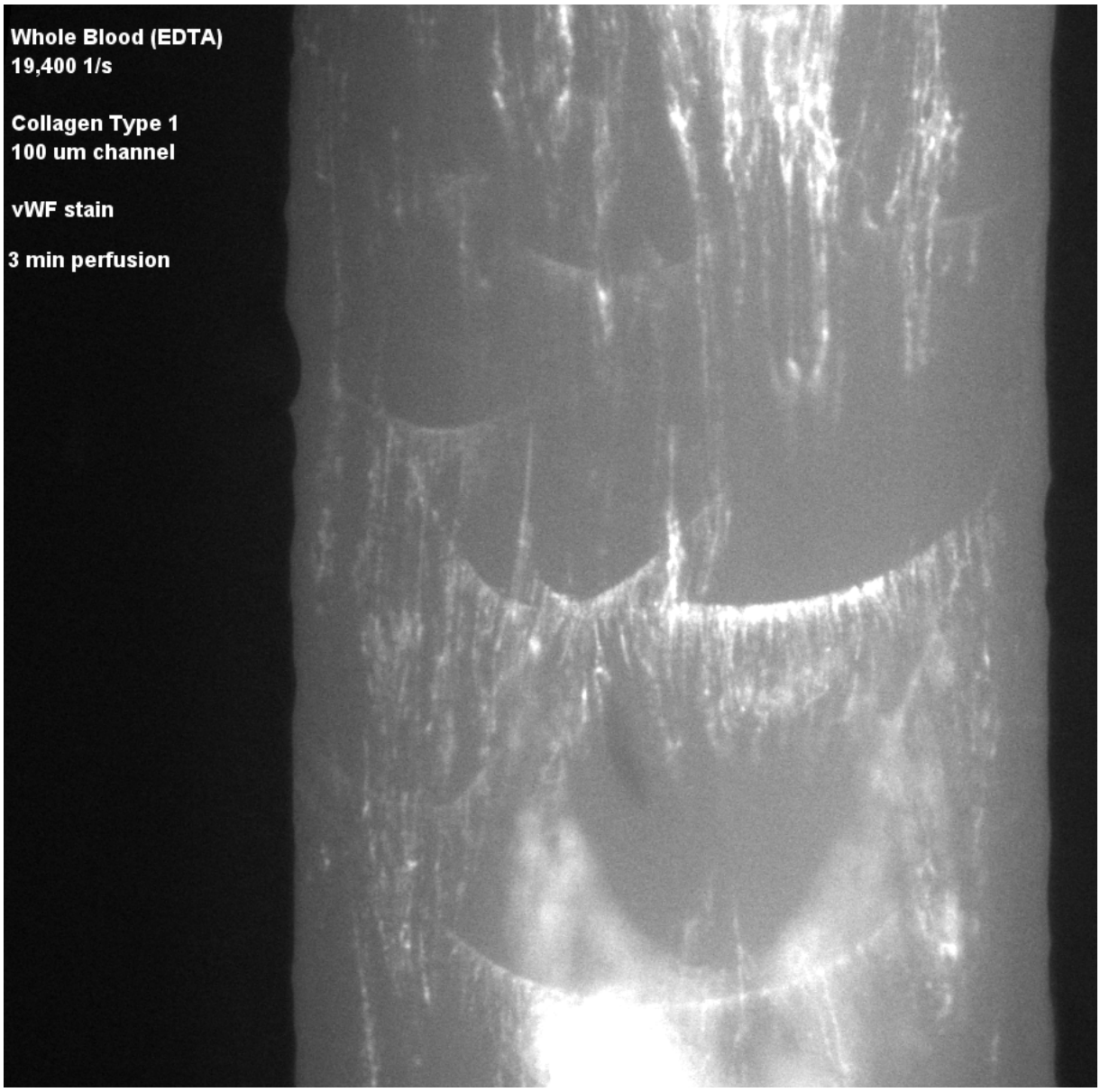

Supplemental Movie M1 vWF fiber deposition under whole blood flow in the absence of Ca^{2+} (EDTA) at 19,400 s^{-1} on a collagen type 1 surface, without stenosis. Flow is from top to bottom.

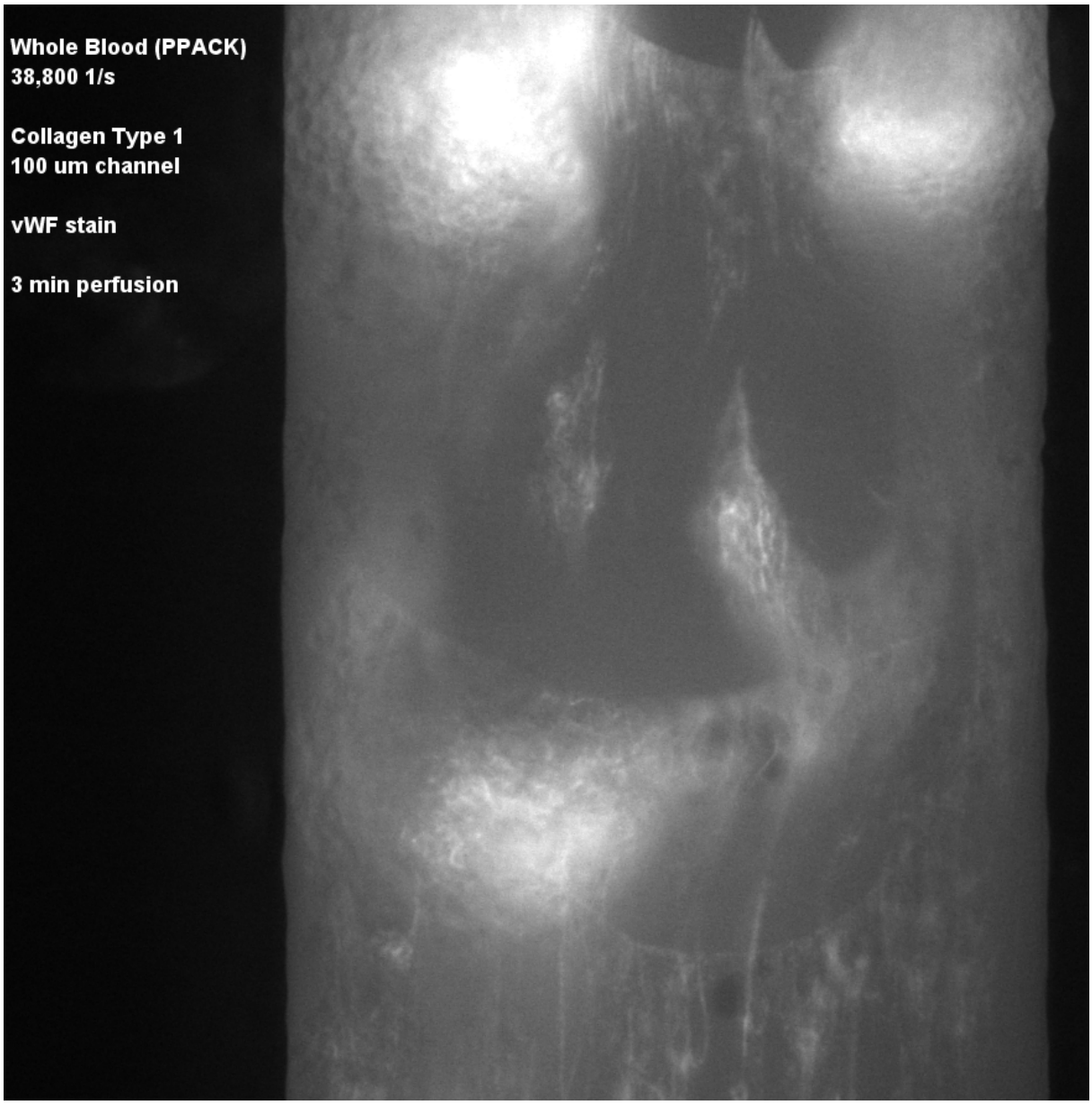

Supplemental Movie M2 vWF fiber deposition under whole blood flow in the presence of Ca^{2+} and PPACK at 38,800 s^{-1} on a collagen type 1 surface, without stenosis. Flow is from top to bottom.